Communication: Direct comparison between theory and experiment for correlated angular and product-state distributions of the ground-state and stretching-excited O(3P) + CH4 reactions

Gábor Czakó

Communication: Direct comparison between theory and experiment for correlated angular and product-state distributions of the ground-state and stretching-excited O(^{3}P) + CH$_4$ reactions

Gábor Czakó[a)]
Laboratory of Molecular Structure and Dynamics, Institute of Chemistry, Eötvös University, H-1518, P. O. Box 32, Budapest 112, Hungary

Motivated by a recent experiment [H. Pan and K. Liu, J. Chem. Phys. **140**, 191101 (2014)], we report a quasiclassical trajectory study of the O(^{3}P) + CH$_4$($v_k = 0, 1$) → OH + CH$_3$ [$k = 1$ and 3] reactions on an *ab initio* potential energy surface. The computed angular distributions and cross sections correlated to the OH($v = 0, 1$) + CH$_3$($v = 0$) coincident product states can be directly compared to experiment for O + CH$_4$($v_3 = 0, 1$). Both theory and experiment show that the ground-state reaction is backward scattered, whereas the angular distributions shift toward sideways and forward directions upon antisymmetric stretching (v_3) excitation of the reactant. Theory predicts similar behavior for the O + CH$_4$($v_1 = 1$) reaction. The simulations show that stretching excitation enhances the reaction up to about 15 kcal/mol collision energy, whereas the O + CH$_4$($v_k = 1$) reactions produce smaller cross sections for OH($v = 1$) + CH$_3$($v = 0$) than those of O + CH$_4$($v = 0$) → OH($v = 0$) + CH$_3$ ($v = 0$). The former finding agrees with experiment and the latter awaits for confirmation. The computed cold OH rotational distributions of O + CH$_4$($v = 0$) are in good agreement with experiment. © 2014 AIP Publishing LLC. [http://dx.doi.org/10.1063/1.4884387]

Since the first measurement of correlated angular and vibrational product distributions for the F + CD$_4$ → DF(v) + CD$_3$(v) reaction reported by Liu and co-workers[1] in 2003, there have been many correlated experiments on the F, Cl, and O(^{3}P) + methane reactions, which extended our knowledge on polyatomic reactivity.[2–4] Very recently the O(^{3}P) + methane reaction received a lot of attention, since we reported the first full-dimensional *ab initio* potential energy surface (PES) for this reaction in 2012 (Ref. [5]) and Espinosa-García and co-workers[6] developed a new PES in 2014. These PESs have recently been used for quasi-classical trajectory (QCT) and reduced-dimensional quantum dynamics computations.[7–10] In 2014 an experimental study also appeared investigating the effects of the antisymmetric stretching excitation on the angular distributions of the O(^{3}P) + CH$_4$($v_3 = 0, 1$) reactions.[11] The experiment found that the angular distributions are backward scattered for the ground-state reaction and shift toward sideways and forward directions upon stretching excitation. However, a recent theoretical study found very similar backward scattering for both the O + CH$_4$($v = 0$) and O + CH$_4$($v_3 = 1$) reactions.[8] This "disagreement" between theory and experiment inspires the present QCT study. Before we move forward, we must realize that the former theoretical study reported angular distributions for the OH($v = 0$) + CH$_3$(all states) channel of both the O + CH$_4$($v = 0$) and O + CH$_4$($v_3 = 1$) reactions, whereas experiment probed the O + CH$_4$($v = 0$) → OH($v = 0$) + CH$_3$($v = 0$) and O + CH$_4$($v_3 = 1$) → OH($v = 1$) + CH$_3$($v = 0$) reactions. Therefore, in this study we compute the correlated product-state specific angular distributions, thereby allowing

direct comparison between theory and experiment. Furthermore, we report predictions for the symmetric-stretching-excited O + CH$_4$($v_1 = 1$) reaction, for which experiment is planned,[11] and provide OH rotational distributions, which can be directly compared to experiment[12] in the case of O + CH$_4$($v = 0$).

Computational details: Full-dimensional QCT calculations are performed on the Czakó–Bowman *ab initio* PES[5] for the O(^{3}P) + CH$_4$($v_k = 0, 1$) → OH + CH$_3$ [$k = 1$ and 3] reactions, where v_1 and v_3 are the symmetric and antisymmetric stretching modes, respectively. The initial conditions are the same as in Ref. [8]. In brief, standard normal-mode sampling is employed, the orientation of CH$_4$ is randomly sampled, b is scanned from 0 to 5 bohrs with a step size of 0.5 bohr (unless otherwise noted), and 5000 trajectories are run at each b; thus, the total number of trajectories is 55 000 for each collision energy (E_{coll}). The product vibrational state specific distributions are computed based on the procedure described in detail in Ref. [13]. The key steps of the polyatomic product analysis are as follows: (1) normal-mode analysis at the equilibrium geometry of CH$_3$, (2) removing the angular momentum by modifying velocities, (3) exact transformation of the Cartesian coordinates and momenta to the Eckart frame, (4) transformation of the Cartesian coordinates and momenta to the normal-mode space using the transformation matrix obtained at step (1), and (5) computation of the harmonic vibrational energy and the corresponding action for each normal mode and rounding each action to the nearest integer value. Then, we use both the standard histogram binning (HB) and the one-dimensional Gaussian binning (1GB)[13–15] methods to calculate product vibrational state specific distributions.
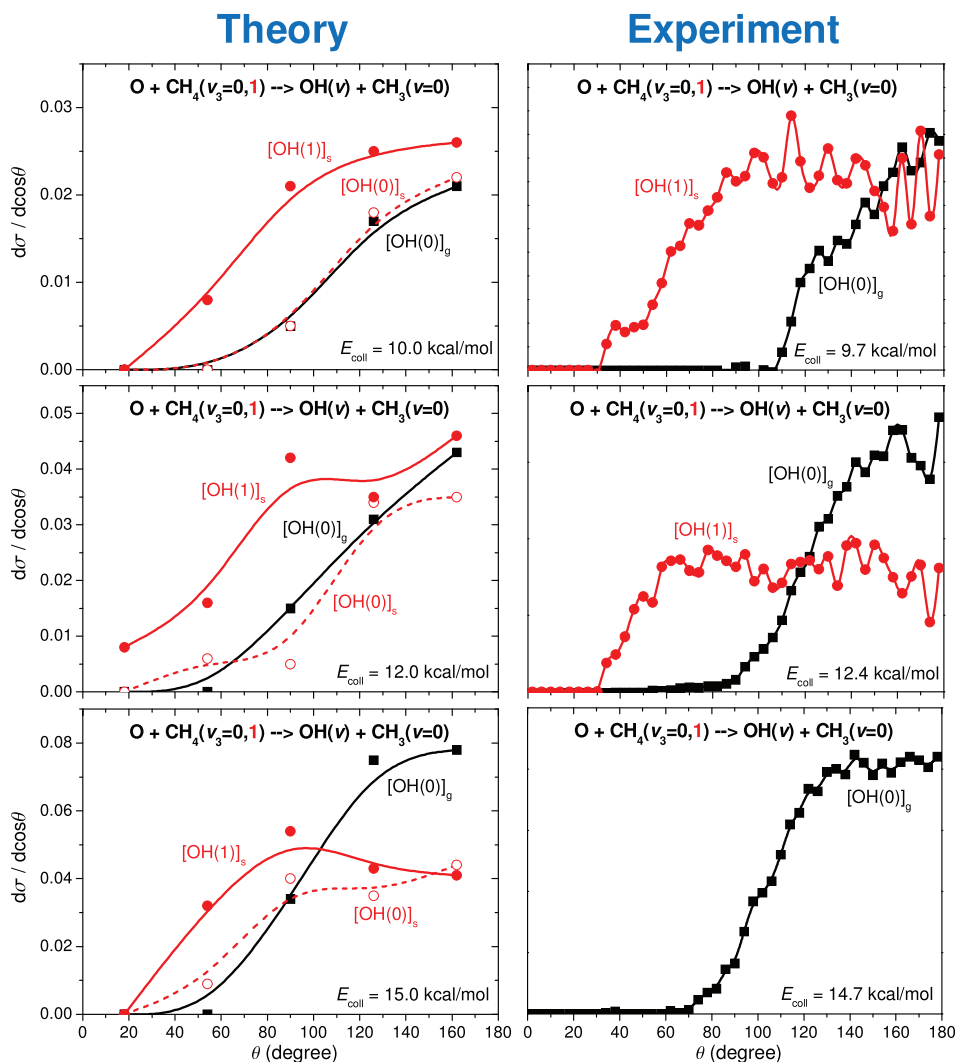
---

a)E-mail: czako@chem.elte.hu

140, 231102-1

FIG. 1. Correlated angular distributions for the ground-state (g) and antisymmetric-stretching-excited (s) $O(^3P)$ + $CH_4(v_3 = 0, 1) \rightarrow OH(v = 0, 1)$ + $CH_3(v = 0)$ reactions. The QCT results are obtained by HB. The experimental data are taken from Refs. 11 and 16.

Angular distributions: The comparison between computed and measured[11] product-state-specific angular distributions for the $O(^3P)$ + $CH_4(v_3 = 0, 1) \rightarrow OH(v = 0, 1)$ + $CH_3(v = 0)$ reactions is shown in Figure 1. As seen, the computed angular distributions for the ground-state reaction are backward scattered indicating a direct rebound mechanism in excellent agreement with experiment. For the stretching-excited reaction both the $OH(v = 0)$ and $OH(v = 1)$ channels are open and experiment reports the angular distributions for $OH(v = 1)$ + $CH_3(v = 0)$. The QCT computations show that the angular distributions of $OH(v = 0)$ + $CH_3(v = 0)$ from $O + CH_4(v_3 = 1)$ are very similar to those of the ground-state reaction. However, for the $OH(v = 1)$ + $CH_3(v = 0)$ channel theory shows that the angular distributions shift toward sideways and forward directions in agreement with experiment. Thus, as found previously for O + CHD_3,[4,5] stretching excitation enlarges the reactive cone of acceptance for the $O + CH_4$ reaction. Another interesting feature of the measured angular distributions is the fact that stretching excitation increases the populations at sideways and forward directions, whereas the backward scattered

reactivity decreases relative to that of the ground-state reaction as the collision energy increases. The QCT results also show this feature, though the crossing of the $OH(v = 0)$ and $OH(v = 1)$ angular distribution curves appears at slightly higher collision energies (Figure 1). The angular distributions of the symmetric-stretching-excited $O(^3P)$ + $CH_4(v_1 = 1)$ reaction are similar to those of the $O(^3P)$ + $CH_4(v_3 = 1)$ reaction as shown in Figure 2. Experimental data have not been available for this reaction yet, but, according to Ref. 11, these measurements are planned in the near future.

Excitation functions: Cross sections for the $O(^3P)$ + $CH_4(v_k = 0, 1) \rightarrow OH(v = 0, 1)$ + $CH_3(v = 0)$ [k = 1, 3] reactions as a function of E_{coll} are shown in Figures 2 and 3. For the $O + CH_4(v = 0)$ and $O + CH_4(v_3 = 1)$ reactions experimental data are available in the 8–15 and 8–13 kcal/mol E_{coll} ranges, respectively, as shown in Figure 3.[11,16] In the experimental E_{coll} range, theory shows that stretching excitation enhances the reaction by a factor of 1.5–3 in quantitative agreement with experiment. Furthermore, both theory and experiment show that translational energy is more efficient in promoting the reaction than vibrational energy.
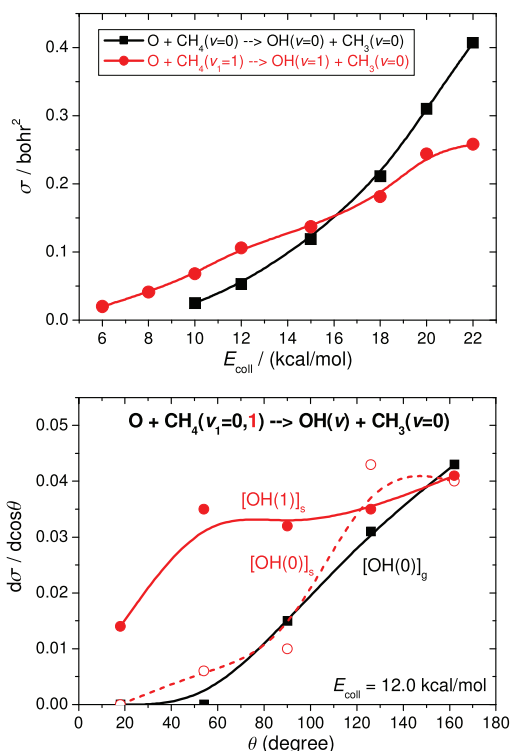
FIG. 2. Correlated cross sections and angular distributions for the ground-state (g) and symmetric-stretching-excited (s) $O(^3P) + CH_4(v_1 = 0, 1) \rightarrow OH(v = 0, 1) + CH_3(v = 0)$ reactions obtained by HB.

Theory gives the excitation functions up to 22 kcal/mol and shows that at around $E_{coll} = 15$ kcal/mol the excitation functions cross each other and the cross sections of the ground-state reaction become larger than those of the stretching-excited reaction. This crossing occurs for both the $O + CH_4(v_1 = 0, 1)$ and $O + CH_4(v_3 = 0, 1)$ reactions and both HB and 1GB give similar excitation functions. (Since getting absolute cross sections from 1GB is problematic due to the issue of assigning weights for non-reactive trajectories, we report the HB cross sections in Figs. 2 and 3. Furthermore, in Ref. 8 we found that HB gives good agreement with quantum mechanical cross sections for the ground-state and stretching-excited $O + CH_4 \rightarrow OH$(all states) + CH_3(all states) reactions.) It is important to note that this crossing
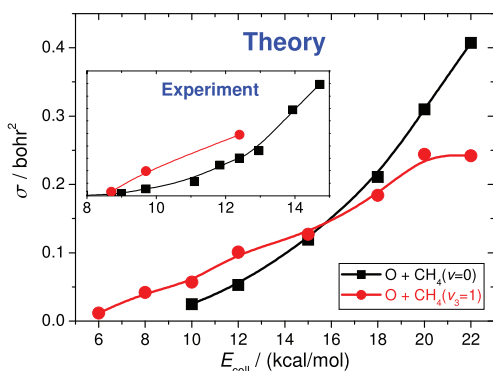

FIG. 3. Correlated cross sections for the ground-state and antisymmetric-stretching-excited $O(^3P) + CH_4(v_3 = 0, 1) \rightarrow OH(v = 0, 1) + CH_3(v = 0)$ reactions. The QCT results are obtained by HB. The experimental data are taken from Refs. 11 and 16.

feature disappears if we sum over all the product states as was done in Refs. 7 and 8. This behavior can be explained by the fact that QCT predicts a decreasing fraction of $CH_3(v = 0)$ from the stretching-excited reactions as E_{coll} increases, whereas the fraction of $CH_3(v = 0)$ slightly increases with E_{coll} for the ground-state reaction.[8] The correlated experiments also suggest this crossing feature if one extrapolates the excitation functions (Fig. 3). The present study may inspire further experiments to verify this behavior. One can also compare the computed and experimental reaction thresholds, which agree well for $O + CH_4(v = 0)$, whereas QCT underestimates it for $O + CH_4(v_3 = 1)$ even if 1GB is used. The latter may be explained by unphysical energy flow to the reaction coordinate near the transition state, which may increase the reactivity especially at low E_{coll}.

Vibrational distributions: Computed OH vibrational distributions correlated to $CH_3(v = 0)$ for the $O(^3P) + CH_4(v_k = 0, 1)$ [$k = 1, 3$] reactions as a function of E_{coll} are given in Figure 4. For $O + CH_4(v = 0)$ standard HB gives about 70% $OH(v = 0)$ and 30% $OH(v = 1)$ without significant E_{coll} dependence. HB obviously overestimates the fraction of $OH(v = 1)$, because the $OH(v = 1)$ channel is energetically not available up to $E_{coll} = 12.6$ kcal/mol. This can happen due to the zero-point energy (ZPE) violation of CH_3, which leaves more energy for OH. 1GB, which handles the ZPE issue of QCT, provides basically 100% population for $OH(v = 0)$ in the entire E_{coll} range up to 22 kcal/mol, in good agreement with experiment. For the $O + CH_4(v_k = 1)$ reactions HB gives inverted OH vibrational distributions, i.e., about 60% $OH(v = 1)$, 30% $OH(v = 0)$, and 10% $OH(v = 2)$. 1GB closes the $OH(v = 2)$ state and decreases the fraction of $OH(v = 1)$. At low E_{coll} $OH(v = 1)$ remains the dominant product and as E_{coll} increases the fraction of $OH(v = 0)$ increases on the expense of $OH(v = 1)$. It is important to note that the OH vibrational distributions of the stretching-excited reactions are significantly colder if we sum over all the product states of CH_3.

Rotational distributions: Vibrationally resolved OH rotational distributions for the $O(^3P) + CH_4(v_k = 0, 1)$ [$k = 1, 3$] reactions at $E_{coll} = 15.0$ kcal/mol are shown in Figure 5. For the $O + CH_4(v = 0)$ reaction, where experimental data (Ref. 12) are also available for comparison, we employ a *b* step size of 0.125 bohr in order to get improved statistics and show QCT results obtained by considering (a) all the trajectories, (b) ZPE constraint applied to the CH_3 product, (c) soft ZPE constraint discarding trajectories if the sum of the product vibrational energies is less than the sum of their ZPEs, and (d) 1GB. Without ZPE constraint the OH rotational distributions are too hot and 1GB does not significantly improve the results of (a), whereas (b) and (c) provide similar cold distributions in reasonably good agreement with experiment (Fig. 5 left panel). Since (b) gives perhaps the best agreement with experiment we show the QCT results obtained by (b) for the $O + CH_4(v_k = 1) \rightarrow OH(v = 0, 1) + CH_3$ [$k = 1, 3$] reactions. The distributions for the v_1- and v_3-mode-excited reactions are very similar. For these reactions both the $OH(v = 0)$ and $OH(v = 1)$ states are open and the corresponding rotational distributions are very different, i.e., $OH(v = 0, N)$ is significantly broader and hotter than $OH(v = 1, N)$. The $OH(v = 0)$ rotational distribution of the ground-state reaction

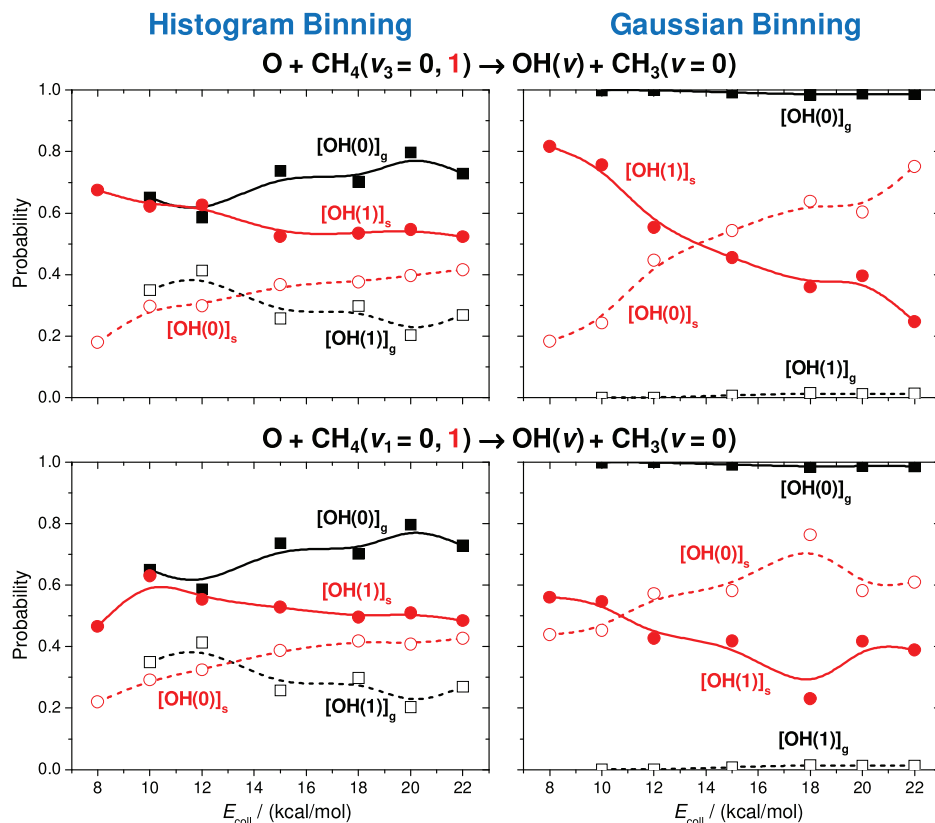FIG. 4. Correlated OH vibrational distributions for the ground-state (g), antisymmetric-stretching-excited (s: $v_3 = 1$), and symmetric-stretching-excited (s: $v_1 = 1$) O(^{3}P) + CH$_4$ reactions as a function of collision energy obtained by different binning techniques.

is colder and hotter than OH($v = 0, N$) and OH($v = 1, N$) of the stretching-excited reactions, respectively. This shows that a part of the stretching-excitation energy of CH$_4$ transfers into the rotational energy of OH($v = 0$). The colder OH($v = 1, N$) distributions from O + CH$_4$($v_k = 1$) relative to OH($v = 0, N$) from O + CH$_4$($v = 0$) may be expected, since the vibrational energy of OH($v = 1$), i.e., 3803 cm^{-1}, is significantly higher than the v_1 (3017 cm^{-1}) and v_3 (3143 cm^{-1}) fundamentals of CH$_4$.

The correlated product-state specific experiments of Liu and co-workers[1–4] have challenged theory for many years. The present theoretical study shows that QCT is capable to reproduce many experimental features if one uses an accurate PES and calculates those product-state specific distributions that can be directly compared to experiment.
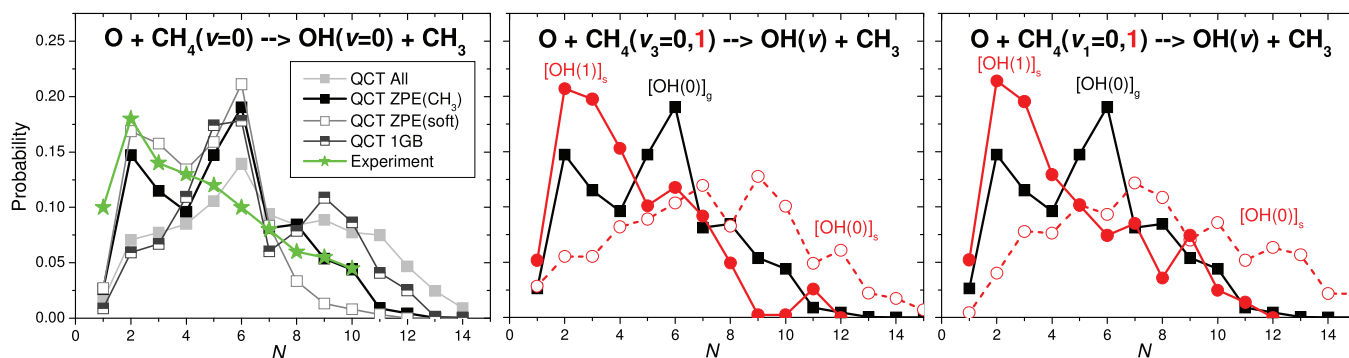
FIG. 5. OH rotational distributions for the ground-state (g), antisymmetric-stretching-excited (s: $v_3 = 1$), and symmetric-stretching-excited (s: $v_1 = 1$) O(^{3}P) + CH$_4$ reactions at collision energy of 15.0 kcal/mol. The QCT data in the left panel are obtained by using (a) all trajectories without ZPE constraint or weighting, (b) CH$_3$-based, (c) soft ZPE constraints (trajectories are discarded if (b) the CH$_3$ product has less vibrational energy than its ZPE and (c) the sum of the product vibrational energies is less than the sum of their ZPEs), and (d) 1GB (product of the vibrational-energy-based weights of OH and CH$_3$). The data shown in the middle and right panels are obtained by (b). The experimental data are taken from Ref. 12. Note that N is defined as the sum of the rotational and orbital ($L = 1$) angular momentum quantum numbers.

[1] J. J. Lin, J. Zhou, W. Shiu, and K. Liu, Science **300**, 966 (2003).
[2] W. Zhang, H. Kawamata, and K. Liu, Science **325**, 303 (2009).
[3] S. Yan, Y.-T. Wu, B. Zhang, X.-F. Yue, and K. Liu, Science **316**, 1723 (2007).
[4] F. Wang and K. Liu, Chem. Sci. **1**, 126 (2010).
[5] G. Czakó and J. M. Bowman, Proc. Natl. Acad. Sci. USA **109**, 7997 (2012).
[6] E. González-Lavado, J. C. Corchado, and J. Espinosa-García, J. Chem. Phys. **140**, 064310 (2014).
[7] R. Liu, M. Yang, G. Czakó, J. M. Bowman, J. Li, and H. Guo, J. Phys. Chem. Lett. **3**, 3776 (2012).
[8] G. Czakó, R. Liu, M. Yang, J. M. Bowman, and H. Guo, J. Phys. Chem. A **117**, 6409 (2013).
[9] E. Gonzalez-Lavado, C. Rangel, and J. Espinosa-García, Phys. Chem. Chem. Phys. **16**, 8428 (2014).
[10] W. Yan, F. Meng, and D. Y. Wang, J. Phys. Chem. A **117**, 12236 (2013).
[11] H. Pan and K. Liu, J. Chem. Phys. **140**, 191101 (2014).
[12] G. M. Sweeney, A. Watson, and K. G. McKendrick, J. Chem. Phys. **106**, 9172 (1997).
[13] G. Czakó, J. Phys. Chem. A **116**, 7467 (2012).
[14] G. Czakó and J. M. Bowman, J. Chem. Phys. **131**, 244302 (2009).
[15] L. Bonnet and J. Espinosa-García, J. Chem. Phys. **133**, 164108 (2010).
[16] J. Zhang and K. Liu, Chem. Asian J. **6**, 3132 (2011).